hygiene

MDPI

Article

Comparison of the Proteome of *Staphylococcus aureus* Planktonic Culture and 3-Day Biofilm Reveals Potential Role of Key Proteins in Biofilm

Md. Arifur Rahman [1,*], Ardeshir Amirkhani [2], Durdana Chowdhury [1], Karen Vickery [1] and Honghua Hu [1,*]

[1] Surgical Infection Research Group, Faculty of Medicine, Health and Human Sciences, Macquarie University, Sydney 2109, Australia
[2] Australian Proteome Analysis Facility, Macquarie University, Sydney 2109, Australia
* Correspondence: md-arifur.rahman2@hdr.mq.edu.au (M.A.R.); helen.hu@mq.edu.au (H.H.)

Abstract: *Staphylococcus aureus* and coagulase-negative staphylococci account for about 80% of infections associated with medical devices and are associated with increased virulence due to their ability to form biofilm. In this study, we aimed to construct a comprehensive reference map followed by significant pathway analysis in the proteome of *S. aureus* biofilm grown for 3 days compared with 24 h of planktonic culture using a high-resolution Tandem Mass Tag (TMT)-based MS. We identified proteins associated with secondary metabolites, ABC transporters, biosynthesis of amino acids, and response to stress, and amino sugar and nucleotide sugar metabolism were significantly upregulated in 3-day biofilm. In contrast, proteins associated with virulence factors, microbial metabolism in diverse environments, secondary metabolites, translation, and energy metabolism were significantly downregulated. GO functional annotation indicated that more proteins are involved in metabolic processes, catalytic activity, and binding in biofilm, respectively. Among the significantly dysregulated proteins, hyaluronidase (hysA) in conjunction with chitinase may play a significant role in the elimination and/or prevention of biofilm development. This study advances the understanding of the *S. aureus* subproteome, identifying potential pathways significant to biofilm biology. The insights gained may aid in developing new therapeutic strategies, including antibiofilm agents, for treating biofilm-related infections associated with implantable medical devices.

Keywords: *Staphylococcus aureus*; biofilms; proteomics; TMT-MS; virulence factors; biosynthetic processes; stress responses

Citation: Rahman, M.A.; Amirkhani, A.; Chowdhury, D.; Vickery, K.; Hu, H. Comparison of the Proteome of *Staphylococcus aureus* Planktonic Culture and 3-Day Biofilm Reveals Potential Role of Key Proteins in Biofilm. *Hygiene* **2024**, *4*, 238–257. https://doi.org/10.3390/hygiene4030020

Academic Editor: Günter Kampf

Received: 20 May 2024
Revised: 23 June 2024
Accepted: 26 June 2024
Published: 3 July 2024

1. Introduction

The Gram-positive opportunistic pathogen *S. aureus* represents a serious public health burden worldwide, particularly within healthcare settings where it is often associated with increased virulence due to its ability to form biofilm. To establish infection, bacteria initially have to attach to the tissue. *S. aureus* does this using Microbial Surface Components Recognising Adhesive Matrix Molecules, abbreviated as MSCRAMMs, and Secreted Expanded-Repertoire Adhesive Molecules, termed SERAMs. In addition, various types of enzymes are also produced by *S. aureus*, including exotoxins such as exfoliative toxins A and B (which increase host tissue invasion), lipases, proteases, thermonucleases, and hyaluronidases [1]. Planktonic cells (free-floating) generally cause acute infections by producing extracellular enzymes and secreted toxins [2]. In chronic infections, *S. aureus* plays a significant role in chronic infections due to its biofilm development on host tissues or implantable medical devices (e.g., prosthetic joints, catheters, breast implants, and pacemakers) [3–6], often withstanding therapeutic intervention.

Biofilms are microbial communities embedded in a self-produced EPS matrix that can be found on any surface [7,8]. Although the exact composition of EPS differs between

various bacterial species and environmental conditions, EPS consists mainly of polysaccharides, proteins, and extracellular DNA (eDNA) [7]. In general, biofilm development is characterised by three stages: initial attachment, biofilm maturation, and dispersal. Several studies have primarily highlighted the elucidation of individual molecular variables that are essential in the growth of *S. aureus* biofilms. A study by Graf et al. (2019) mentioned some of the proteinaceous and non-proteinaceous factors responsible for various phases of biofilm formation and the synthesis and expression of these molecular factors are closely regulated by several biofilm regulators such as AgrA and RNAIII, Rot, SigB, SarA, IcaR, CodY, and others [9].

Attempts to comprehend the biochemical framework of biofilm formation and resilience have constantly demonstrated alterations in the protein expression profile in *S. aureus* [10–14] compared with planktonic counterparts.

Numerous studies have been conducted on the total proteome of *S. aureus* biofilm; however, there is no effective technique for the early identification of biofilms, which poses numerous challenges to developing efficient therapeutic interventions [15]. Hence, numerous facets of the complex structure and role of biofilms have yet to be elucidated. Therefore, continuous improvement in the field of proteomics such as high-resolution TMT-MS [16] and associated database enrichment has been shown to be a strong instrument for gaining deeper molecular insight into biofilms and later diseases.

In the present study, we aimed to construct a comprehensive proteomic reference map of *S. aureus* biofilm compared with planktonic culture by employing TMT-based high-resolution MS. In addition, potential marker proteins were identified and further characterised to better understand the potential role(s) of key proteins in *S. aureus* biofilm biology.

2. Materials and Methods

This research aimed to develop a quantitative proteomic analysis to delineate the differences between *S. aureus* cells transitioning between planktonic and biofilm conditions. To achieve this goal, we performed protein extraction, fractionation, reduction, alkylation, and in-solution digestion, generating samples for analysis using TMT-based MS. Each growth condition—planktonic and biofilm—was examined with three biological replicates.

2.1. Microorganism and Culture Conditions

Staphylococcus aureus reference strain (ATCC 25923) was cultured to stationary phase in 100% tryptic soy broth (TSB) for 24 h, maintaining constant agitation at 130 rpm and 37 °C. To produce a 3-day biofilm, *S. aureus* was cultivated as previously described [17]. Briefly, biofilm formation occurred on removable polycarbonate coupons within a Centers for Disease Control (CDC) biofilm reactor (BioSurface Technologies Corp, Bozeman, MT, USA) under batch conditions at 37 °C. Initially, 50% TSB was used for 48 h, after which the media was exchanged with 20% TSB every 48 h as needed to achieve a 3-day biofilm. Shear force was induced by baffle rotation at 130 rpm. The biofilms were cultivated and harvested across three independent experiments.

2.2. Protein Extraction and Fractionation

Protein extraction and fractionation were performed as previously described [17]. Concisely, planktonic bacteria were pooled from three separate growth samples of 24 h cultures of *S. aureus* and then mixed with a lysis buffer composed of 100 mM Triethylammonium bicarbonate (TEAB; Sigma-Aldrich, St. Louis, MO, USA) at pH 8.5, along with 1% (*w*/*v*) sodium deoxycholate (Sigma-Aldrich) at a ratio of 10 parts supernatant to 1 part lysis buffer. As for the *S. aureus* biofilm, the growth of 3-day biofilm-coated coupons (n = 24) were washed to remove non-adherent cells, and then each coupon was placed individually in 2 mL of phosphate-buffered saline (PBS) and lysis buffer, followed by an overnight incubation with gentle shaking at 4 °C. The samples underwent probe sonication in an ice-cold environment (using Sonic Ruptor, Omni International, Kennesaw, GA, USA) for 2 min at 50% power and 70% pulses. Following this, the samples were centrifuged at 12,000× g for

10 min, and the supernatant was then passed through a 10 kDa molecular weight cut-off (MWCO) ultra-membrane filter tube (Sigma-Aldrich) prior to another centrifugation step at 4000× *g* for 20 min. Protein samples underwent three washes with PBS to remove TSB and lysis buffer and were subsequently concentrated using a 3 kDa MWCO filter tube (Sigma Aldrich).

The protein concentration was measured using the BCA protein assay (Thermo Fisher Scientific, Waltham, MA, USA) at a wavelength of 562 nm by following the manufacturer's instructions and measuring the absorbance.

2.3. Protein Reduction, Alkylation, and Digestion

Protein reduction, alkylation, and digestion were performed as previously described [17]. Concisely, a total of 40 µg of protein was reduced (5 mM DTT, 15 min, RT), alkylated (10 mM IAA in darkness, 30 min, RT), and then diluted with 100 mM of TEAB, pH 8.5. The in-solution digestion step was carried out overnight at RT with Lys-C and trypsin at a ratio of 1:30, respectively, for 5.5 h at 37 °C. Further sample preparation steps included an adjustment to 1% (*v*/*v*) TFA and removal of precipitated deoxycholate by centrifugation; then, the sample was centrifuged at 14,100× *g* and desalted with 0.2% TFA washing by utilising SDB-RPS (3M-Empore) Stage Tips (Thermo Fisher Scientific). The elution of samples was carried out using 5% ammonium hydroxide in 80% acetone, followed by centrifugation at 1000× *g* for 5 min. Subsequently, the samples were vacuum-dried and stored at −20 °C until further processing.

2.4. TMT Labeling and High pH Fractionation

TMT labelling and high pH fractionation were performed as previously described [17]. Concisely, TMT (Thermo Fisher Scientific) reagents (0.8 mg) were dissolved in 85 µL of acetone, and 41 µL of this solution was added to the reconstituted samples (100 µL of 100 mM TEAB pH 8.5) and then incubated for 1 h at RT. Each TMT-labelled sample was mixed with 8 µL of hydroxylamine (5%) and then incubated for 15 min at RT. A volume of 2 µL of each labelled sample was pooled, vacuum-dried, and then reconstituted in a 30 µL solution of FA (0.1%) (Merck, Kenilworth, NJ, USA). The mixture was centrifuged for 5 min at 14,000× *g* and subsequently analysed using a mass spectrometer.

Data searching was performed using Proteome Discoverer 1.3 (for detailed information, refer to the data processing section). Utilizing the normalization values derived from this search result, an equivalent number of peptides were taken from each sample, pooled, and then vacuum-dried using a miVac concentrator. The dried labelled sample was reconstituted in buffer A (5 mM ammonia, pH 10.5) and fractionated by high pH RP-HPLC (Agilent Technologies, Santa Clara, CA, USA). The dried labelled sample was reconstituted in buffer A. Following sample loading and a 10 min wash with 97% buffer A, the concentration of buffer B (5 mM ammonia solution with 90% acetone, pH 10.5) was ramped up from 3% to 30% over 55 min, then maintained at 70% for 10 min, and finally raised to 90% for 5 min, all at a flow rate of 300 µL/min. The eluent was collected at 2 min intervals initially, up to 16 min, and then at 1 min intervals for the rest of the gradient. The fractionated sample was divided into 19 fractions, dried using a miVac concentrator, and subsequently resuspended in 55 µL of FA (0.1%) for MS analysis.

2.5. Nanoflow LC-ESI-MS/MS

The following steps were performed as previously described [17].

2.5.1. Nanoflow LC-ESI-MS/MS Using Orbitrap Elite

Data acquisition was performed using an Orbitrap Elite mass spectrometer (Thermo Fisher Scientific, Dreieich, Germany, and USA) coupled with a PicoView 550 Nanospray Source (New Objectives, Littleton, CO, USA) and an Eksigent UPLC system (AB SCIEX, Framingham, MA, USA) comprising an ekspert™ nanoLC 425 UPLC pump and an ekspert™ nanoLC 400 autosampler (Thermo Fisher Scientific) was utilized for the ex-

periment. Each fraction, totalling 20 µL, was loaded onto a self-packed trap column measuring 100 µm × 3.5 cm with a Halo® 2.7 µm 160 Å ES-C18 (Advanced Materials Technology, Wilmington, DE, USA). The desalting process was conducted using a loading buffer [0.1% FA] at a flow rate of 4 µL/min for 10 min. The elution of peptides was achieved through linear gradients of mobile phase A (0.1% FA/5% DMSO) and mobile phase B (0.1% FA/5% DMSO). The gradient was initiated with the following phases: B (1–10%, 0.1 min), B (10–20%, 52 min), and B (20–32%, 48 min), followed by (32–43%, 20 min) at a flow rate of 450 nL/min throughout the gradient. Before reaching the analytical column, the eluent from the trap underwent dilution with buffer A at a flow rate of 100 nL/min. Subsequently, the peptides underwent refocusing and separation on the analytical column maintained at 60 °C. Peptides were ionized by electrospray ionization, and data-dependent MS/MS acquisition was performed by utilising an Orbitrap Elite (Thermo Fisher Scientific) comprising 1 full MS1 (R = 120 K) scan acquisition from 380 to 1600 m/z and 15 HCD type MS2 scans (R = 30 K).

2.5.2. Nanoflow LC-ESI-MS/MS Using Q Exactive

Data acquisition was performed using a Q Exactive (Thermo Fisher Scientific) Mass Spectrometer equipped with Nano Spray Source and Easy nLC 1000 (Thermo Fisher Scientific). Each fraction, totalling 10 µL, was loaded onto a self-packed trap column measuring 100 µm × 3.5 cm with a Halo® 2.7 µm 160 Å ES-C18 (Advanced Materials Technology, Wilmington, DE, USA). The desalting process was conducted using a loading buffer [0.1% FA] followed by peptides that were eluted with the linear gradients of mobile phase A (0.1% FA) and buffer B [100% (v/v) acetone, 0.1% (v/v) FA]. The gradient was initiated with the following phases: B (1–30%, 110 min) and B (30–85%, 2 min), followed by B (85%, 8 min) with a flow rate of 300 nL/min throughout the gradient. Peptides were ionized by electrospray ionization and data-dependent MS/MS acquisition was performed by utilising a Q-Exactive consisting of 1 full MS1 (R = 70 K) scan acquisition from 350 to 1850 m/z and 10 HCD type MS2 scans (R = 70 K).

2.6. Database Search, Statistical Analysis, and Bioinformatics

A database search, statistical analysis, and bioinformatics analysis were performed according to a recent publication [17]. Concisely, the raw data files were submitted to Proteome Discoverer (v 1.3, Thermo Fisher Scientific) and the processing of the data was conducted using Sequest and Mascot (Matrix Science, London, UK) against the *S. aureus* reference strain (ATCC 25923) sourced from Genbank CP009361 and CP009362. Protein identification utilised the following parameters: peptide mass tolerance set at 10 ppm; MS/MS tolerance at 0.1 Da; enzyme = trypsin, missed cleavage = 1; fixed modification, carbamidomethyl ©, TMT10-plex (K), and TMT10-plex (N-term); and variable modification, oxidation (M), deamination (N, Q), and acetylation (N-Terminus). Quantification was carried out as per the peak intensities of reporter ions in the MS/MS spectra. Peptide identification utilised a threshold of less than 1% false discovery rate. Protein quantification was determined by the total intensity of the assigned peptides. Following the extraction of protein ratios through Proteome Discoverer, further processing and statistical analyses were conducted utilising the TMTPrePro R package. Afterwards, the BLAST search was executed using highly annotated strains *S. aureus* N315 and *S. aureus* COL. In the context of biofilm growth versus planktonic growth, proteins were deemed upregulated when the TMT ratio > 1.5, while those with a TMT ratio < 0.66 were considered downregulated with a significant p-value < 0.05. Proteins exhibiting significant differential expression (>2-fold) were identified using VENNY (v.2.1) (https://bioinfogp.cnb.csic.es/tools/venny/, accessed on 25 June 2018) and subjected to further processing to obtain deeper functional insights. The functional pathways of the significantly identified proteins were analysed utilising the KEGG mapper (https://www.genome.jp/kegg/mapper/, accessed on 6 August 2018). Subcellular localisation of the significantly identified proteins was assessed using PSORTb (v 3.0.2) (http://www.psort.org/psortb/index.html, accessed on 23 January 2018). The PPI

network of the significantly differentially regulated proteins was examined using STRING-db (v 10.0) (http://string-db.org/, accessed on 25 June 2018). Identification of virulence factors was performed using the Virulence Factors of Pathogenic Bacteria Database (VFDB) (http://www.mgc.ac.cn/VFs/, accessed on 15 March 2019).

2.7. Validation of TMT Data with qPCR Results

qPCR was performed to validate the TMT data as previously described [17]. To validate the expression variances between planktonic and biofilm states, we selected five genes: Hyaluronidase HysA, Chitinase SA0914, Glutamyl endopeptidase sspA, Pyruvate carboxylase pyc, and Succinate dehydrogenase sdhB as targets to analyse the levels of RNA expression. The 16S rRNA served as the internal control for data normalisation and compared the differential expression levels of the five genes between the planktonic culture and 3-day biofilm samples.

RNA extraction from *S. aureus* planktonic culture and 3-day biofilm samples was carried out using a RNeasy Mini Kit (Qiagen, Hilden, Germany). To prevent degradation, RNAlater was utilised, and RNase-free DNase treatment was employed to eliminate genomic DNA. The RNA concentration was measured by absorbance at 260 nm, while its quality was evaluated based on the absorbance ratio (A260/A280). A total of 200 ng of RNA was used for cDNA synthesis, facilitated by the SuperScript™ IV VILO™ Master Mix (Thermo Fisher Scientific). The real-time (RT)-PCR primers utilized in this study (Table S1) were designed based on the genome sequences of *S. aureus* (ATCC 25923), accessible through Genbank accession numbers CP009361 and CP009362.

Quantitative real-time PCR (qPCR) was performed using an Applied Biosystems quantitative real-time PCR machine (ViiA™ 7 qPCR, ThermoFisher Scientific). Each experiment was conducted in duplicate using two biological replicates. The qPCR reaction mix, totalling 25 µL, comprised 12.5 µL of 2× PowerUp™ SYBR™ Green Master Mix (Thermo Fisher Scientific), 1 µL each of 10 µM reverse and forward primers (resulting in a final primer concentration of 400 nM), 8.5 µL of water, and 2 µL of 1:5 diluted cDNA. Each PCR run included a no-template control (NTC) and a no-reverse transcription control (no-RT control). The NTC contained all PCR components except the cDNA template, which was replaced by nuclease-free water. The no-RT control involved the cDNA sample without the reverse transcriptase enzyme to check for contaminating genomic DNA in the RNA. The cycling conditions for RT-PCR commenced with an initial activation step at 95 °C for 10 min to activate the polymerase. This was followed by 40 cycles comprising denaturation at 95 °C for 15 s, annealing at either 50 °C or 55 °C for 40 s, and extension at 72 °C for 30 s, or alternatively, annealing and extension at 60 °C for 1 min.

Initially, the expressed copy number of each target gene was normalised to the copy number of 16S rRNA within the same growth condition. Subsequently, the levels of candidate gene expression in the planktonic culture and 3-day biofilm samples were compared to investigate relative gene expression, employing a previously described method [18]. The ratios derived from the qPCR results were obtained by comparing them with the planktonic culture and 3-day biofilm samples.

3. Results

3.1. TMT Identification of Differentially Regulated Proteins in the Biofilm

In this study, a total of 1636 non-redundant proteins, each with at least one unique peptide and less than 1% false discovery rate, were identified and quantified. The profile of differentially expressed proteins in a 3-day biofilm was depicted using a volcano plot by implementing the fold change (>1.5-fold) and *p*-value (<0.005) cut-off values (Figure 1A). Of these, 273 proteins were significantly ($p < 0.05$) differentially regulated exclusive proteins (DREPs) greater than 2-fold change during biofilm growth in comparison to planktonic bacteria (Figure 1B). These 273 DREPs could be regarded as potential variables responsible for the difference in the proteome of biofilm compared with planktonic growth as depicted in the Venn diagram (Figure 1B). Of these, 82 proteins were upregulated (Figure 1B, Table S2)

and 191 were downregulated in the biofilm (Figure 1B, Table S3). Of the upregulated biofilm proteins, 35 proteins (42.7%) were associated with recognised protein pathways (Figure 1B). Similarly, 74 (38.7%) of the downregulated biofilm proteins were associated with recognised protein pathways (Figure 1B). In this study, we identified 313 commonly regulated proteins between 3-day biofilm and planktonic mode of growth (results not shown). Among the DREPs, we identified a total of 34 hypothetical proteins and hypothetical protein KQ76_04110 had the highest differential expression being upregulated 5.09-fold. We identified a molybdenum ABC transporter permease (4.68-fold upregulated) and transport of molybdenum via ABC transporter into the cells is essential for bacterial growth [19]. Further, we identified DNA-directed RNA polymerase subunit omega (4.50-fold), which is involved in RNA polymerase, pyrimidine, and purine metabolism; glycosyltransferase (4.32-fold); and branched-chain amino acid transporter II carrier protein (4.04-fold).

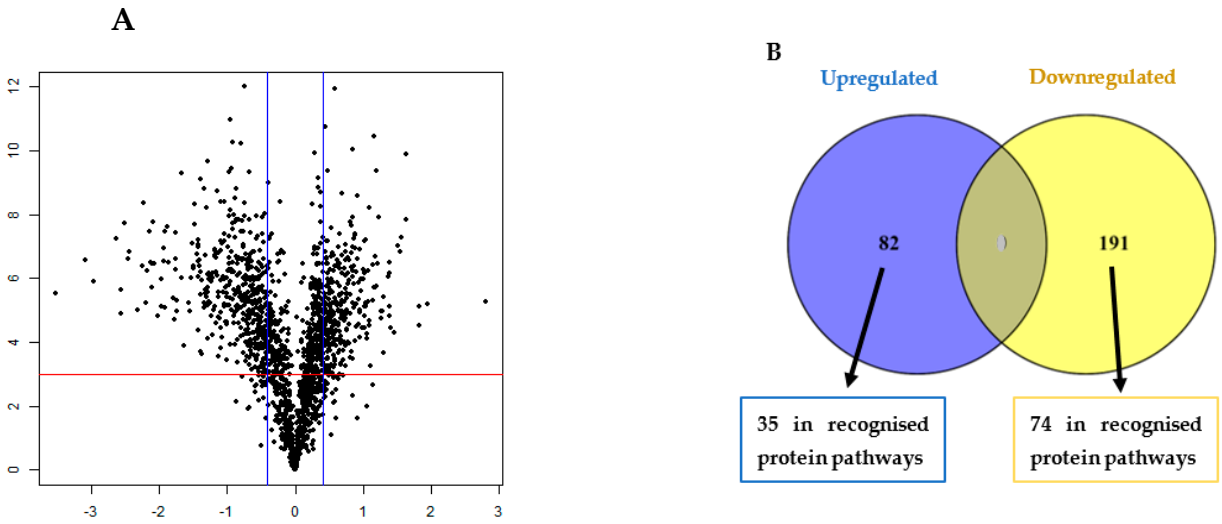

Figure 1. The volcano plot illustrates the distribution of the protein expression profile differences within the 3-day biofilm (**A**). The *Y*-axis, displayed as −log 10, signifies the *p*-value, where a higher numerical value indicates a lower *p*-value and thus higher credibility. On the *X*-axis, the fold change (log2) of differentially expressed proteins is depicted by blue lines, with two vertical blue lines marking fold changes of −1.5 and +1.5. Consequently, the dots positioned above the red line on the positive side signify proteins significantly upregulated ($p < 0.05$), while those on the negative side denote proteins significantly downregulated ($p < 0.05$). (**B**) This Venn diagram represents identified proteins dysregulated (>2-fold, $p < 0.05$) within the 3-day biofilm. The diagram shows the dispersion of 273 upregulated and downregulated proteins of which there were 82 upregulated and 191 downregulated proteins identified in the 3-day biofilm. We identified 313 commonly regulated proteins between 3-day biofilm and planktonic mode of growth (results not shown). Pathway analysis was performed using KEGG.

The most downregulated protein was delta-hemolysin (−34.02-fold), which is involved in quorum sensing. Delta-hemolysin is a small amphipathic membrane-damaging virulence factor protein that showed potential antimicrobial activity. Delta-hemolysin may act either by binding to the surface of the cell and aggregating to form transmembrane pores, thus destabilising the cytoplasmic membrane by affecting the membrane curvature, or function as a detergent by solubilising the membrane at higher concentrations [20]. Significant downregulation of delta-hemolysin may prevent the dispersal of cells, thereby enhancing biofilm formation.

Spermidine/putrescine ABC transporter substrate-binding protein (potD) was also downregulated 22.02-fold and functions in the ABC transporter pathway. PotD is a periplasmic substrate-binding protein that binds extracellular polyamines (e.g., spermidine and putrescine), and binding of spermidine to PotD is essential for building a more compact protein structure and cell growth. PotD negatively regulates the spermidine-preferential

uptake system transcription of the operon, thereby a decrease in spermidine uptake activity leads to increased polyamine accumulation in cells [21,22]. In addition, extracellular proteins including alpha-hemolysin (−13.82-fold), phosphodiesterase (−12.33-fold), cysteine protease (−11.44-fold), and transglycosylase (−10.14-fold) were also downregulated. Several ribosomal proteins were also downregulated (Table S3). Moreover, we identified 20 virulence factor proteins using VFDB among the DREPs (Table 1).

3.2. GO Analysis and Annotation of Differentially Regulated Proteins in the Biofilm

We performed GO functional annotation for all DREPs. PANTHER assessment showed the involvement of 12 distinct classes of proteins in the entire global repository of proteins (Figure 2). Nucleic acid-binding proteins (20.7%), hydrolases and transferases (17.2%), ligases (13.8%), transcription factors (8.6%), and oxidoreductases (6.9%) were the most prominent classes.

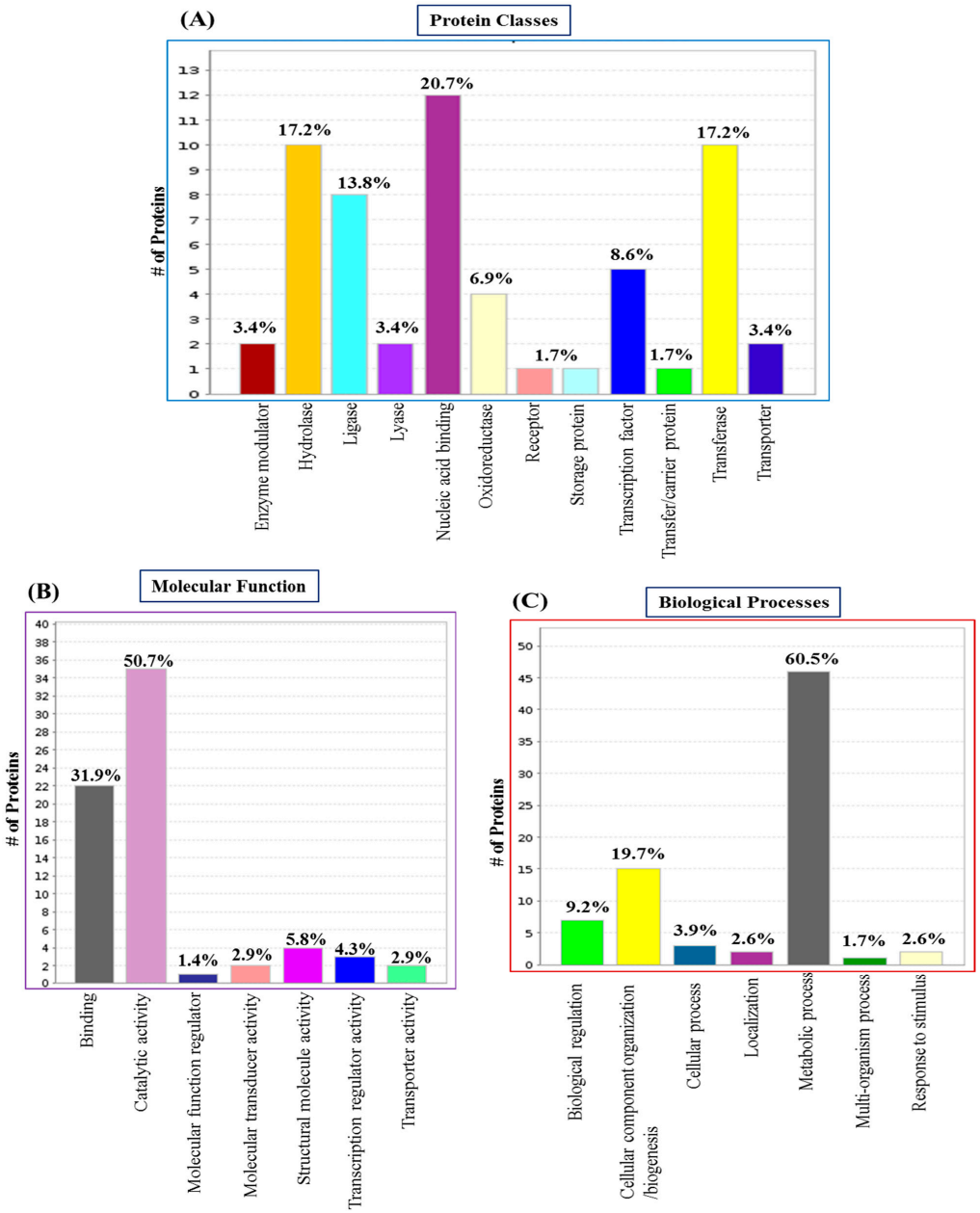

Figure 2. Classification of the DREPs of *S. aureus* biofilm using Gene Ontology based on their functional annotations. (**A**) GO Protein Classes; (**B**) GO Molecular Function; and (**C**) GO Biological Processes.

Table 1. List of the exclusively differentially expressed virulence factor proteins identified by VFDB in *S. aureus* biofilm in comparison to planktonic culture (fold change > 2, $p < 0.05$). * CM denotes cytoplasmic membrane.

Function	Accession ID	Uniprot ID	Virulence Factors	Related Genes	Fold Change	Protein Pathway	Subcellular Localization
Adherence	AIO22275.1	Q7A382	Clumping factor B	clfB	−2.96	*S aureus* infection	Cell wall
	AIO22136.1	Q7A3J7	Fibronectin-binding protein A	fnbA SA2291	−2.60	Bacterial invasion of epithelial cells	Cell wall
	AIO19779.1	A0A0H2X057	Immunoglobulin G binding protein A	spa SACOL0095	−4.71	*S aureus* infection	Cell wall
	AIO20229.1	Q5HIB2	Serine-aspartate repeat-containing protein E	sdrE SACOL0610	−3.82	*S aureus* infection	Cell wall
	AIO20228.1	Q7A780	Serine-aspartate repeat-containing protein D	sdrD SA0520	−4.49	*S aureus* infection	Cell wall
Toxins	AIO20763.1	A0A0H3JMC2	Alpha-hemolysin	SA1007	−13.83		Extracellular
	AIO22369.1	Q5HEI1	Phospholipase C (EC 3.1.4.3) (beta-hemolysin) (beta-toxin) (sphingomyelinase) (SMase)	hlb SACOL2003	−12.33	Quorum sensing, inositol phosphate metabolism, glycerophospholipid metabolism, biosynthesis of secondary metabolites	Extracellular
	AIO21667.1	P0A0M2	Delta-hemolysin (delta-lysin) (delta-toxin)	hld SA1841.1 SAS065	−34.02	Quorum sensing	Extracellular
	AIO22060.1	Q7A3S2	Gamma-hemolysin component C	hlgC SA2208	−3.79	*Staphylococcus aureus* infection	Extracellular
	AIO20093.1	A0A0H3JSX3	Exotoxin 11 (superantigen-like protein)	set11	−3.63	*Staphylococcus aureus* infection	Extracellular
Antiphagocytosis (capsule)	AIO19823.1	A0A0H3JKC9	Capsular polysaccharide synthesis enzyme Cap5G	capG	2.018	Amino sugar and nucleotide sugar metabolism	Cytoplasmic

Table 1. *Cont.*

Function	Accession ID	Uniprot ID	Virulence Factors	Related Genes	Fold Change	Protein Pathway	Subcellular Localization
Exo-enzyme	AIO21508.1	Q5HEW4	Serine protease SplE	splE	−4.18	Quorum sensing	Extracellular
	AIO21601.1	P65826	Cysteine proteinase A	scpA	−3.73		Extracellular
	AIO20644.1	Q5HH36	Cysteine proteinase B	sspB	−11.44		Extracellular
	AIO19987.1	Q7A7P2	lipase	geh	−4.12		Extracellular
	AIO21839.1	A0A0H3JN21	Hyaluronate lyase	hysA	2.50		Extracellular
	AIO20645.1	Q5HH35	Glutamyl endopeptidase	sspA	−6.52	Quorum sensing	Extracellular
	OOC94232.1	A0A0H2WZZ4	Aureolysin	aur	−3.22	*Staphylococcus aureus* infection, cationic antimicrobial peptide (CAMP) resistance	Extracellular
	AIO19888.1	A0A0H3JNG8	Staphylocoagulase	coa	2.10		Extracellular
Secretion system (type VII secretion system)	AIO19949.1	Q7A7S3	Type VII secretion protein EsaA	esaA SA0272	−2.29		CM *

The molecular function categories by PANTHER revealed the seven most represented molecular functions (Figure 2). The maximum number of proteins were involved in catalytic activity (50.7%), followed by binding (31.9%) and structural molecule activity (5.8%). Upon assessing biological processes, we identified the seven most represented biological processes (Figure 2). Of these, metabolic processes are the most prevalent biological processes, representing 60.5% of the protein repository followed by cellular component organisation or biogenesis (19.7%), biological regulations (9.2%), and cellular processes (3.9%).

3.3. Significantly Dysregulated Proteins and Pathway Analysis in the Biofilm

We analysed the TMT results using KEGG pathways to establish pathways impacted by bacterial biofilm formation in *S. aureus*. We annotated 289 DREPs using the KEGG database, with all data mapped onto 113 recognised pathways. Among these, 35 out of 82 significantly upregulated proteins were involved in recognised pathways. The 35 exclusively upregulated proteins were mainly involved in the biosynthesis of secondary metabolites; biosynthesis of amino acids; microbial biosynthesis of antibiotics; metabolism in diverse environments; ABC transporters; alanine, aspartate, and glutamate metabolism; amino sugar and nucleotide sugar metabolism; purine metabolism; ribosome and pyrimidine metabolism; arginine biosynthesis, tyrosine and tryptophan biosynthesis, etc. (Figure 3). In addition, upregulated proteins were also found to be involved in energy metabolisms such as glycolysis and galactose, and synthesis of cell wall components such as peptidoglycan biosynthesis.

On the other hand, 74 out of 191 significantly downregulated proteins were involved in recognised pathways. KEGG pathway analysis revealed that the 74 exclusively downregulated proteins were mainly involved in quorum sensing, the citrate cycle (TCA cycle), carbon metabolism, pyruvate metabolism, aminoacyl-tRNA biosynthesis, cationic antimicrobial peptide (CAMP) resistance, methane metabolism, glycerophospholipid metabolism, two-component systems, etc. (Figure 3).

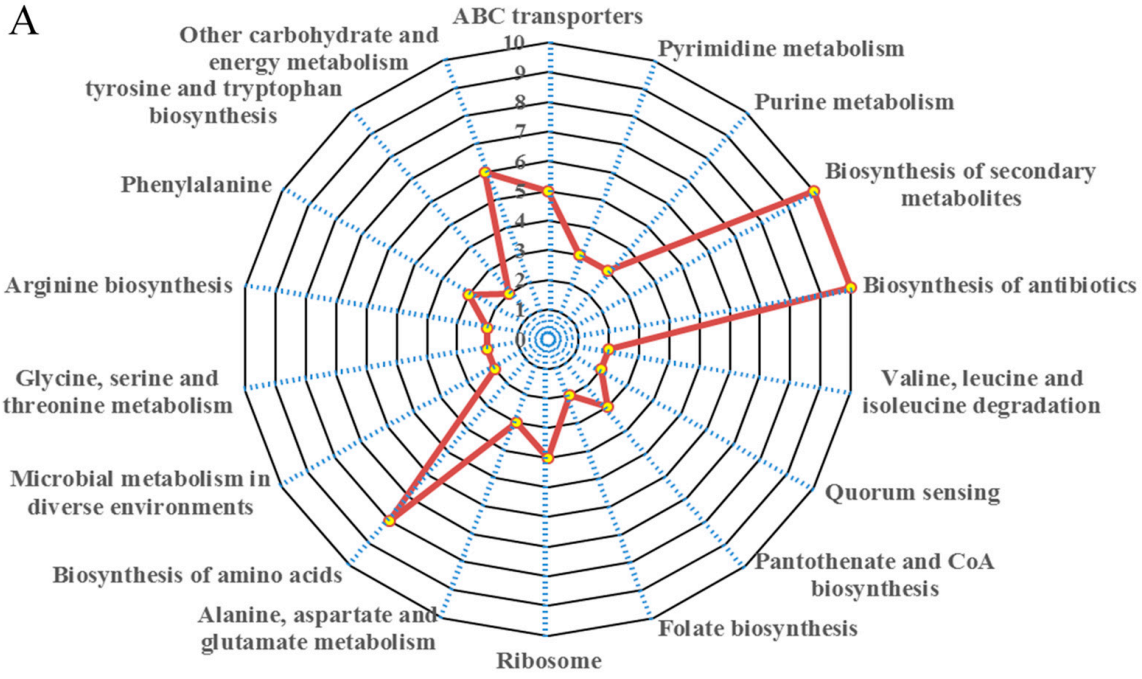

Figure 3. *Cont.*

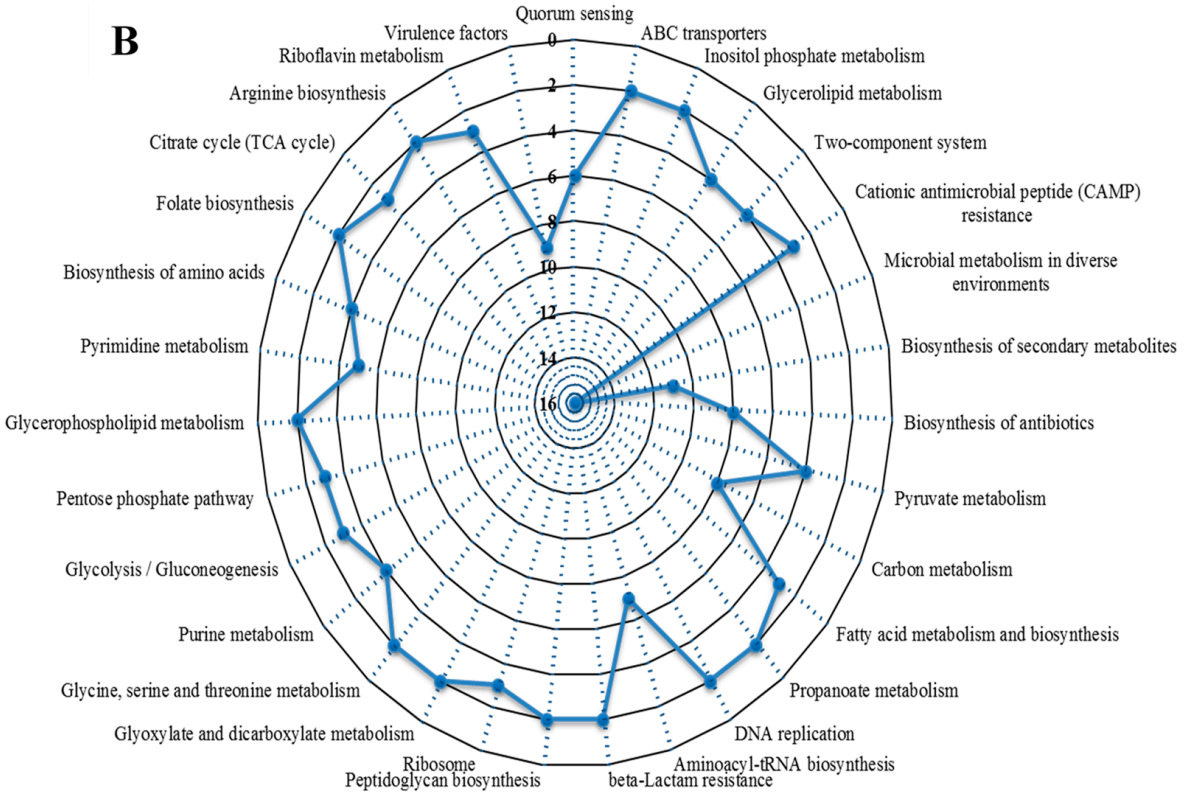

Figure 3. The DREPs of *S. aureus* biofilm showed functional diversity using KEGG pathway analysis. (**A**) major pathways involved in exclusively upregulated proteins; (**B**) major pathways involved in exclusively downregulated proteins.

3.4. Protein–Protein Interaction (PPI) Analysis in the Biofilm

We established protein–protein interaction (PPI) networks using STRING software (v 10.0) to assess the network of those proteins identified exclusively to be expressed differentially in the biofilm mode of growth. In this PPI analysis, all predicted interactions were tagged as "high-confidence" ($\geq$0.7), and nodes not connected to the network in STRING software were omitted. Among the 289 DREPs, 129 nodes (proteins) and 145 edges (interactions) formed the final network (Figure S1).

The PPI network revealed that one protein symbolises a majority of connections: 30S ribosomal protein S5 (rpsE). This protein was found to be upregulated in the biofilm growth mode, could connect with 39 other proteins (Figure S1), and plays an important role in translational accuracy. Among these 39 possible connections, most are involved in metabolic and catalytic activity and binding (such as ion, nucleic acid, metal, and drug binding). The findings of this subnetwork are in line with the top protein classes and biological processes acquired with PANTHER analysis (Figure 2). Further relevant subnetworks consist of nodes associated with gene expression, translation, ATP biosynthesis, virulence factors, glucose metabolism, and stress response (Figure S1).

3.5. Validation of TMT Data with Real-Time qPCR

The qPCR results ratios were derived by comparing them with the planktonic state in the 3-day biofilm. Individual normalised qPCR results are demonstrated in Table S4. The results of both upregulated and downregulated protein and gene expressions were measured in terms of fold change (FC) (Table S4). The qPCR results indicated that the ratios of the levels of gene expression were partially consistent with the data acquired from the TMT-based MS analysis (Table S4).

4. Discussion

Whilst the proteomics of *S. aureus* biofilm have previously been investigated [10,12,14,23], we utilised highly powerful TMT-MS in this study. The TMT-labelling approach, in combination with tandem MS, has the potential to conduct high-resolution analysis of proteins in the low-mass region with the possibility to label up to 10 samples simultaneously [16,24]. This powerful proteomic strategy can be helpful in obtaining a deeper understanding of biological mechanisms as well as the screening of biomarkers by examining the variations in protein expression levels.

We also conducted qPCR experiments on selected significantly dysregulated genes to investigate the correlation between qPCR and TMT data. The gene expression levels measured by qPCR were found to be generally consistent with the TMT-based MS analysis data for some proteins, but not for all. The lack of consistency between transcriptomics and proteomics results is likely due to differences in half-lives and post-transcriptional mechanisms. Additionally, the lack of correlation between TMT and qPCR data could be attributed to variations in cell lysis and extraction methods used for the samples.

A study by Cristian et al. (2021) [25] reported proteomic analysis using *S. aureus* strains to identify the differential expression between planktonic culture and 1-day biofilm and revealed that three of the five upregulated proteins are involved in carbon metabolism or stress response. Notably, alcohol dehydrogenase and 30S ribosomal proteins are associated with antimicrobial resistance mechanisms, specifically detoxification. In contrast, downregulated proteins, including 2,3-bisphosphoglycerate-dependent phosphoglycerate mutase, alkyl hydroperoxide reductase subunit C, ATP-dependent 6-phosphofructokinase, and catalase, are primarily involved in energy- and oxygen-related metabolism [25].

However, in our current study, we identified significantly upregulated proteins associated with ABC transporters and exo-enzymes involved in numerous regulatory pathways. Whereas significantly downregulated proteins were found to be associated with the citrate cycle (TCA cycle), carbon metabolism, pyruvate metabolism, aminoacyl-tRNA biosynthesis, cationic antimicrobial peptide (CAMP) resistance, methane metabolism, etc. This finding is significantly different from the previous studies. This is likely because immature biofilms formed within 24 hr have a more active metabolism and are less complex than more mature biofilms. Further, we found that proteins associated with peptidoglycan biosynthesis, sugar transporters, and amino acid metabolism were upregulated, whereas proteins associated with ABC transporters, DNA replication, and adhesion proteins were downregulated in the 12-day *S. aureus* biofilms [16].

These findings showed the variations in the proteomics profiling and associated regulatory pathways between immature biofilms and more mature biofilms. Therefore, because of the differences found between immature and more mature biofilms in previous studies on *S. aureus*, we chose to measure the changes associated with biofilm formed for 3 days as this is also associated with increased biocide tolerance [26].

In our proteomics data, we identified several proteins associated with transporters; these were mostly ABC transporters (Table S2, Figure 3) uniquely upregulated in the *S. aureus* biofilm state: molybdenum ABC transporter permease (4.68-fold), peptide ABC transporter substrate-binding protein (2.91-fold), spermidine/putrescine ABC transporter ATP-binding protein potA (2.39-fold), heme ABC transporter ATP-binding protein (2.32-fold), and glutamine ABC transporter ATP-binding protein (2.05-fold). Proteins were also exclusively downregulated in biofilm growth and included ABC transporter ATP-binding proteins encoded by vga and iron ABC transporter substrate-binding proteins encoded by SA0691. ATP-binding cassette transporters (ABC transporters) are members of a superfamily of proteins that are transmembrane proteins linked with adenosine triphosphate (ATP)-binding energy utilisation. They play substantial functions in the molecular (macro and micro) uptake of nutrients, such as capsular polysaccharides, small molecule inhibitors, amino acids, lipids, and vitamins. To better understand virulence and drug resistance, microbial ABC transporters are gaining attention as a potential target [27]. In previous studies, ABC transporters (such as ABC transporter lipoprotein, ABC transporter

permease protein, ABC transporter periplasmic amino acid-binding protein, and ABC transporter ATP-binding protein) have been reported to be upregulated in biofilm formation in *S. aureus* [12,28,29] and in numerous other bacteria, including *Cronobacter* sp., *Streptococcus uberis*, *Rhizobium leguminosarum*, *Pseudomonas fluorescens*, and *Bacillus subtilis* [30–34]. ABC transporters have also been reported to be downregulated, such as putative ABC transporter permease in *Listeria monocytogenes* [35] and ABC transporter ATP-binding protein in *S. aureus* [36]. In these instances, the specific role they have (i.e., up- or downregulation) depends on the substrates being supplied by the ABC transporters. Although the exact reason for the downregulation of ABC transporters is yet to be explored, it could be due to the lower metabolic rate of the biofilm; hence, it did not need to transport ATP as much. A study by Brady et al. (2006) revealed the upregulation of a membrane-bound ABC transporter protein in *S. aureus* biofilm growth and suggested that it may be an excellent vaccine candidate, as previous work reported it as immunogenic in *S. aureus* infections in humans [28,37]. Taken together, the unique or exclusive ABC transporter proteins (especially those that are membrane-bound) identified in our study may play an important role in biofilm formation, which may lead to potential marker proteins, vaccines, and antimicrobial targets for biofilm-related infections.

Among the significant differentially regulated proteins in the biofilm extractomes, we identified most of the extracellular or cell-wall-associated proteins to be primarily represented by virulence factors (Table 1). Proteins exclusively upregulated include fibrinogen-binding protein (SA1000), hypothetical protein KQ76_08475 (SA1452), hyaluronate lyase (hysA), and coagulase, while downregulated proteins (Table S3, Figure 3) include hemolysins (hld, SA1007, and hlgCAB), proteases (sspABP, splCEF, SA1121, and clpP), nucleases (nuc, rnhC, SA1526, cbf1, and rnz), peptidases (lytM, SA0205, SA0620, and sspA), lipases (lip1 and lip 2), a chitinase (SA0914), a phenol soluble modulin (SACOL1186), fibronectin-binding protein (fnbA), and adhesin (sasF). Among the upregulated proteins, fibrinogen-binding protein is an MSCRAMM that is vital for the attachment of *S. aureus* to human cells and thus for the spread of infections [38,39]. A recent in vitro study by Kot et al. (2018) demonstrated that the expression levels of fibrinogen-binding protein in a weakly attaching strain of *S. aureus* was considerably smaller than in a strongly attaching strain of *S. aureus* [40]. Studies by Resch et al. (2006) reported the upregulation of fibrinogen-binding protein in biofilm growth mode compared with the planktonic state, which shows a similar trend with our study. In an in vivo rat model of central venous catheter infection using *S. epidermidis*, rats lacking fibrinogen-binding motifs showed more robust biofilm on the catheter, indicating its significance in the in vivo biofilm development [41]. In addition, the binding of *S. aureus* to fibrinogen-binding protein and coagulase demonstrates various evasive responses that protect bacteria against the immune system, and its binding is influenced by Rot- and Agr-mediated regulatory systems [10,41].

Hyaluronidase (hysA) is an extracellular enzyme exclusively upregulated in the biofilm state and plays an important role in disseminating recognised biofilms by the degradation of hyaluronic acid (HA) (Figure 4). HA is an extracellular matrix component that has been revealed to enhance biofilm development in Gram-positive pathogens, including *Streptococcus intermedius* and *Streptococcus pneumoniae*. A very recent in-depth study by Ibberson et al. (2016) demonstrated that *S. aureus* integrates HA into the biofilm matrix both in vivo (murine implant-associated infection model) and in vitro, and HysA acts as a spreading factor by dispersing the biofilm and disseminating bacteria to new locations of infection [42]. On the other hand, among the exclusively downregulated proteins, chitinase (SA0914) is an exo-enzyme involved in quorum sensing that prevents the initial stage development of biofilms. Interestingly, HA is the structural constituent of N-acetyl-D-glucosamine (Figure 4), which can be hydrolysed by chitinase [43]. Therefore, we can speculate that hysA in conjunction with chitinase may play a significant role in the elimination and/or prevention of biofilm development.

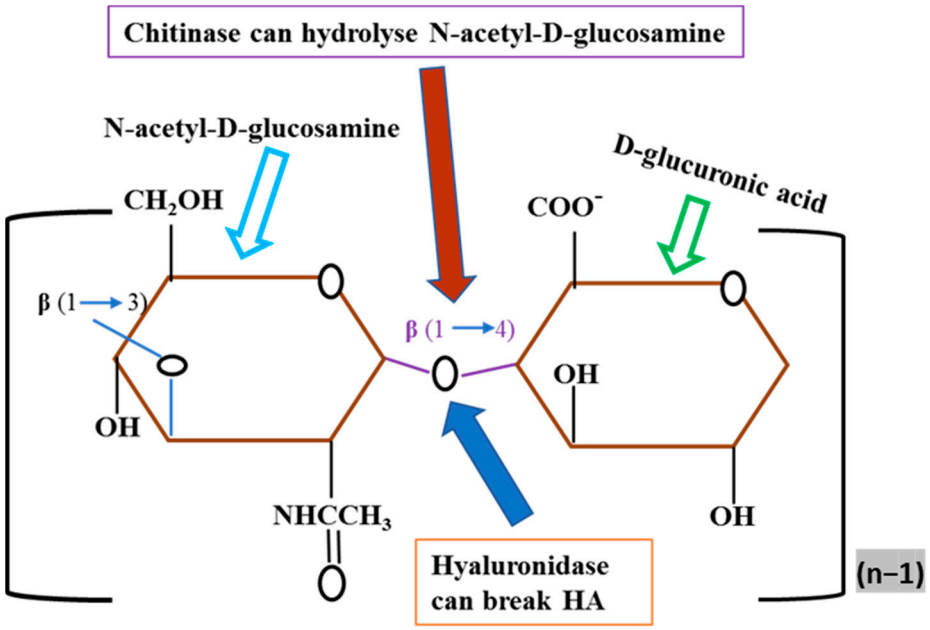

Figure 4. This figure shows a structural component of hyaluronic acid (HA) and the breaking point by significantly identified proteins (HysA and Chitinase). HA comprises repeating disaccharide units of N-acetyl-D-glucosamine and D-glucuronic acid, and the units are linked by repeating glycosidic bonds beta-1,4 and beta-1,3.

Further, the significant downregulation of virulence-related and cell wall proteins showed that the bacteria adapted to the diverse biofilm condition by reducing some less essential roles such as adhesion, invasion, and virulence. For example, an agr quorum-sensing system regulates the expression of virulence genes and contributes to the dispersal and structuring of biofilms by regulating extracellular proteases (e.g., sspAB) and phenol-soluble modulin (PSM) surfactant peptides [44,45]. Further, the Staphylococcal accessory regulator (SarA) is a positive biofilm regulator through the downregulation of extracellular nuclease (nuc) and proteases [2,3]. Downregulation of these genes from our findings shows similarity with the findings of Resch et al. [46]. Studies have shown that *S. aureus* produces proteases, which in most cases act as a virulence factor that may influence the chronicity of *S. aureus* infections [47]. In vivo, the inflammatory response itself also contributes to tissue destruction by continually recruiting proinflammatory cells such as lymphocytes and macrophages, releasing proteases and inflammatory mediators [4]. Although proteases help dislodge biofilms, they also harm ordinary and curative tissues, whereas macrophages may form a fibrous capsule around the implants [4].

Further pathway analysis revealed that the upregulation of glyceraldehyde-3-phosphate dehydrogenase encoded by gapA1 (2.34-fold), cystathionine gamma-synthase encoded by metB (2.33-fold), threonine synthase encoded by thrC (2.27-fold), argininosuccinate lyase encoded by argH (2.21-fold), acetolactate synthase encoded by alsS (2.21-fold), argininosuccinate synthase encoded by argG (2.15-fold), 3-phosphoshikimate 1-carboxyvinyltransferase encoded by aroA (2.09-fold), and histidinol–phosphate aminotransferase encoded by SACOL2701 (2.01-fold) are involved in the biosynthesis of amino acid (Table S2 and Figure 3). Besides protein parts, amino acids function as signals for gene expression molecules and regulators. In the meantime, changes in the metabolism of amino acids contribute to the development of biofilms in vitro and in vivo catheter infections [48,49]. Studies by Ammons et al. (2014) reported that, in addition to the diverse role of amino acids in biofilm development, they are also involved in substantial energy expenditure for adequate redox equilibrium maintenance, cell wall synthesis components, and deposition of the EPS matrix [13]. Notably, in our biofilm extractomes, we found exclusively upregulated proteins involved in amino sugar and nucleotide sugar metabolism (such as glmS, nanE, and capG),

which is linked with peptidoglycan biosynthesis (Figure 5). As we know, peptidoglycan is the major component of the bacterial cell wall, and our study also observed a significant accumulation of peptidoglycan biosynthesis-associated protein (e.g., murA). Therefore, we can speculate that the proper utilisation of amino acids will stimulate cell wall formation, leading to EPS matrix deposition and enhancing biofilm formation.

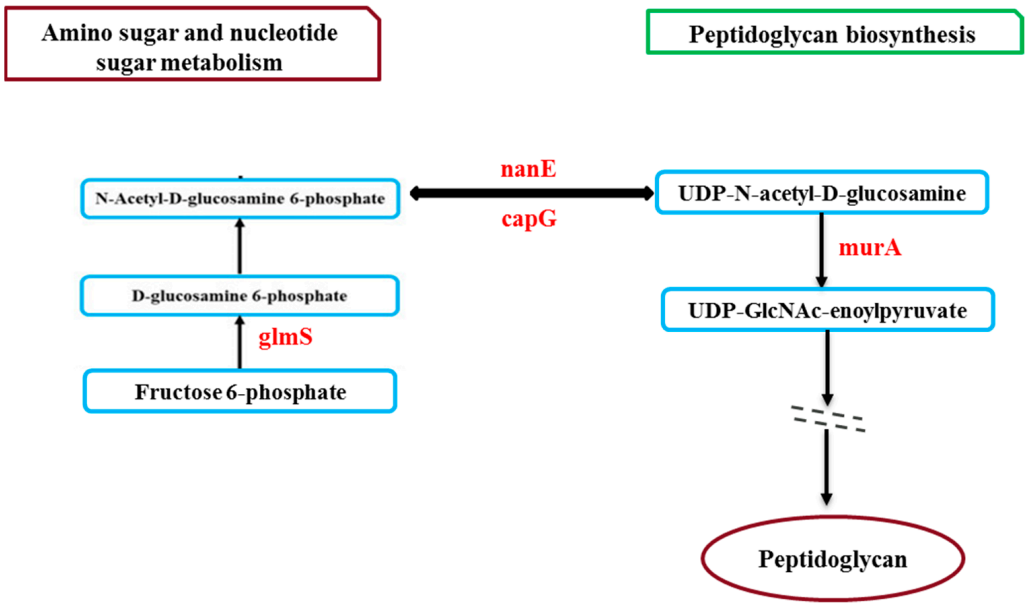

Figure 5. Pathway demonstration showing exclusively upregulated proteins (red colour—encoded genes) involved in amino sugar and nucleotide sugar metabolism and linked with peptidoglycan biosynthesis in 3-day biofilm.

Many ribosomal subunit proteins such as 30S ribosomal protein S14 (rpsN), 50S ribosomal protein L27 (rpmA), 30S ribosomal protein S5 (rpsE), and 50S ribosomal protein L10 (rplJ) were exclusively upregulated (Table S2 and Figure 3) under the biofilm growth state, while 50S ribosomal protein L17 (rplQ) and 50S ribosomal protein L20 (rplT) were downregulated (Table S3 and Figure 3). Usually, ribosomal subunit proteins play a significant role in regulating the expression of whole proteins. The 50S proteins involve the activity that catalyses the formation of peptide bonds, protects premature polypeptide hydrolysis, and helps to fold proteins after synthesis, etc. It is stated that synthesising some of the peptides or proteins helps to promote resistance. For example, 50S ribosomal protein L27 (rpmA) plays a critical role in tRNA substrate stabilisation during the peptidyl transfer reaction as well as ribosome assembly and catalysis, even with certain levels of stress environment (e.g., deletion of some part) [50].

Among the significantly differentially regulated proteins, we identified several proteins related to different stress responses in the *S. aureus* biofilm extractomes: DNA-directed RNA polymerase subunit omega (RpoZ), dehydrogenases (e.g., bfmBAA, gap, and ldhD), oxidoreductases (e.g., guaC, SACOL0959, SA0558, and nfrA), reductases (e.g., SACOL1543, SA0759, SACOL1768, and trxB), glutathione S-transferase, and heat shock protein GrpE (Table S3 and Table 1). The formation of a stress response is a significant characteristic of the biofilm life cycle as it leads to changes in many gene expressions, which increase antimicrobial resistance and are generally regulated by alternative RNA polymerase sigma factor B (SigB). Multiple studies have reported increased or decreased expression of stress response-associated proteins in *S. aureus* biofilm [10,12,51] and other bacteria [52–54]. However, notably, we identified a unique DNA-directed RNA polymerase subunit omega (RpoZ), which is 4.52-fold upregulated in the biofilm. Even though very little is known about RpoZ, a very recent study reported its significant roles in stability, complex assembly, maintenance of transcriptional integrity, and cellular physiology in response to stress in *S. aureus*

biofilm [51]. Another protein, glyceraldehyde-3-phosphate dehydrogenase (Gap), was exclusively upregulated in biofilm growth mode and under oxidative stress environments and showed a significant positive correlation between development, ATP level, and Gap activity in planktonic *S. aureus* [55]. Pathway analysis revealed that the Gap, an enzyme involved in multiple pathways (such as biosynthesis of amino acids, carbon metabolism, microbial metabolism in diverse environments, glycolysis/gluconeogenesis, etc.), plays an important role in the phosphorylation of glyceraldehyde-3 phosphate and contributes to phosphotransferase activity and repair apoptosis [56]. Gap is upregulated in biofilms developed by numerous bacterial species [57–61].

The metabolic activity and growth rate of bacteria are affected by changes in the gradient of oxygen and other nutrients within biofilms. Many studies have demonstrated that cells within hypoxic conditions have decreased metabolic activity [62–64]; this slow pace of development suggests tolerance as antimicrobials are most efficient against rapidly developing cells [65–67]. In addition, the deeper layers of cells are also located in biofilms with undergrowth-limiting conditions, with anaerobic or micro-aerobic conditions. Pyruvate fermentation could support these cells, allowing them to survive with little or no oxygen [68]. In our *S. aureus* biofilm extractomes, we observed significant upregulation of acetolactate synthase (alsS), which is responsible for the activation of the butanediol pathway from pyruvate. Activation of this pathway promotes NADH oxidation and indicates that there is a tenuous redox balance during the development of biofilms [69]. Another study reported that alsS utilises pyruvate to produce acetoin, which is essential for acid tolerance within biofilms [70].

Among the 273 DREPs, unique or exclusive proteins identified in *S. aureus* biofilm contain 34 functionally unknown or very little-known hypothetical proteins (Tables S2 and S3), including a hypothetical protein, namely hypothetical protein KQ76_08425, encoded by SA0772 with the highest upregulation (5.09-fold), which suggests that the complex metabolic and regulatory reaction to biofilm is not yet fully elucidated. Even though the role of the hypothetical protein remains unknown, it is likely to play a part in the distinct physiological state of the biofilm. In particular, we can speculate regarding proteins that are exclusively upregulated in the biofilm growth state. Although there have been previous reports of hypothetical proteins implicated in alterations in biofilm [71–73], more research is required to assess their role as these proteins are homologous to conserved hypothetical proteins from other organisms, which include certain pathogenic strains.

In this study, we constructed a comprehensive reference map of the proteome of *S. aureus* biofilm, observed a significant range of abundance variation in the biofilm, identified differentially expressed potential marker proteins, and elucidated potential role(s) of these exclusive proteins using this reference strain. In future studies, identified significant marker proteins, such as virulence factors and antibiofilm agents, will be further characterised and analysed using different platforms (e.g., targeted ELISAs, biochemical assays) to validate the proteomics results in numerous *S. aureus* strains, including clinical strains.

Supplementary Materials: The following supporting information can be downloaded at: https://www.mdpi.com/article/10.3390/hygiene4030020/s1, Figure S1: The network of DREPs of *S. aureus* biofilm was analysed by STRING software (v.10.0); Table S1: Primers used in this study; Table S2: List of the significantly upregulated proteins in *S. aureus* biofilm in comparison to planktonic culture; Table S3: List of the exclusively downregulated proteins in *S. aureus* biofilm in comparison to planktonic culture; Table S4: Relative correlation of selected qPCR gene expression data to TMT protein expression data in 3-day biofilm in comparison to planktonic culture.

Author Contributions: Conceptualization, M.A.R., K.V. and H.H.; methodology, M.A.R., K.V., H.H., A.A. and D.C.; formal analysis, M.A.R., K.V., H.H., D.C. and A.A.; investigation, M.A.R., K.V., H.H. and A.A.; data curation, M.A.R., K.V., H.H. and A.A.; writing—original draft preparation, M.A.R., K.V., H.H. and A.A.; writing—review and editing, M.A.R., K.V., H.H. and A.A.; supervision, K.V. and H.H. All authors have read and agreed to the published version of the manuscript.

Funding: This research received no external funding.

Institutional Review Board Statement: Not applicable.

Informed Consent Statement: Not applicable.

Data Availability Statement: Data are available via ProteomeXchange [74] with the identifier PXD033499.

Acknowledgments: The authors acknowledge the support of an International Macquarie University Research Excellence Scholarship from Macquarie University for M.A.R. We thank Maria Mempin for her kind advice and technical support for this study. We acknowledge the technical support of the Australian Proteome Analysis Facility, Macquarie University. We also thank Dana Pascovici and the team for their great assistance in conducting the biostatistical and bioinformatics analyses at APAF.

Conflicts of Interest: The authors declare no conflicts of interest.

References

1. Tam, K.; Torres, V.J. *Staphylococcus aureus* secreted toxins and extracellular enzymes. *Microbiol. Spectr.* **2019**, *7*, 2. [CrossRef] [PubMed]
2. Lister, J.L.; Horswill, A.R. *Staphylococcus aureus* biofilms: Recent developments in biofilm dispersal. *Front. Cell. Infect. Microbiol.* **2014**, *4*, 178. [CrossRef]
3. Francis, D.; Bhairaddy, A.; Joy, A. The biofilm proteome of *Staphylococcus aureus* and its implications for therapeutic interventions to biofilm-associated infections. *Adv. Protein Chem. Struct. Biol.* **2023**, *138*, 327–400. [PubMed]
4. Ajdic, D.; Zoghbi, Y.; Gerth, D.; Panthaki, Z.J.; Thaller, S. The relationship of bacterial biofilms and capsular contracture in breast implants. *Aesthetic Surg. J.* **2016**, *36*, 297–309. [CrossRef] [PubMed]
5. Barrett, L.; Atkins, B. The clinical presentation of prosthetic joint infection. *J. Antimicrob. Chemother.* **2014**, *69*, i25–i27. [CrossRef]
6. Chatterjee, S.; Maiti, P.; Dey, R.; Kundu, A.; Dey, R. Biofilms on indwelling urologic devices: Microbes and antimicrobial management prospect. *Ann. Med. Health Sci. Res.* **2014**, *4*, 100–104. [PubMed]
7. Karygianni, L.; Ren, Z.; Koo, H.; Thurnheer, T. Biofilm matrixome: Extracellular components in structured microbial communities. *Trends Microbiol.* **2020**, *28*, 668–681. [CrossRef] [PubMed]
8. Vickery, K. Microbial biofilms in healthcare: Formation, prevention and treatment. *Materials* **2019**, *12*, 2001. [CrossRef]
9. Graf, A.C.; Leonard, A.; Schäuble, M.; Rieckmann, L.M.; Hoyer, J.; Maaß, S.; Lalk, M.; Becher, D.; Pané-Farré, J.; Riedel, K. Virulence factors produced by *Staphylococcus aureus* biofilms have a moonlighting function contributing to biofilm integrity. *Mol. Cell. Proteom.* **2019**, *18*, 1036–1053. [CrossRef]
10. Moche, M.; Schlüter, R.; Bernhardt, J.; Plate, K.; Riedel, K.; Hecker, M.; Becher, D. Time-resolved analysis of cytosolic and surface-associated proteins of *Staphylococcus aureus* HG001 under planktonic and biofilm conditions. *J. Proteome Res.* **2015**, *14*, 3804–3822. [CrossRef]
11. Atshan, S.S.; Shamsudin, M.N.; Sekawi, Z.; Lung, L.T.T.; Barantalab, F.; Liew, Y.K.; Alreshidi, M.A.; Abduljaleel, S.A.; Hamat, R.A. Comparative proteomic analysis of extracellular proteins expressed by various clonal types of *Staphylococcus aureus* and during planktonic growth and biofilm development. *Front. Microbiol.* **2015**, *6*, 524. [CrossRef] [PubMed]
12. Islam, N.; Kim, Y.; Ross, J.M.; Marten, M.R. Proteomic analysis of *Staphylococcus aureus* biofilm cells grown under physiologically relevant fluid shear stress conditions. *Proteome Sci.* **2014**, *12*, 21. [CrossRef] [PubMed]
13. Ammons, M.C.B.; Tripet, B.P.; Carlson, R.P.; Kirker, K.R.; Gross, M.A.; Stanisich, J.J.; Copié, V.R. Quantitative NMR metabolite profiling of methicillin-resistant and methicillin-susceptible *Staphylococcus aureus* discriminates between biofilm and planktonic phenotypes. *J. Proteome Res.* **2014**, *13*, 2973–2985. [CrossRef] [PubMed]
14. Resch, A.; Leicht, S.; Saric, M.; Pásztor, L.; Jakob, A.; Götz, F.; Nordheim, A. Comparative proteome analysis of *Staphylococcus aureus* biofilm and planktonic cells and correlation with transcriptome profiling. *Proteomics* **2006**, *6*, 1867–1877. [CrossRef]
15. Kranjec, C.; Morales Angeles, D.; Torrissen Mårli, M.; Fernández, L.; García, P.; Kjos, M.; Diep, D.B. Staphylococcal biofilms: Challenges and novel therapeutic perspectives. *Antibiotics* **2021**, *10*, 131. [CrossRef] [PubMed]
16. Rahman, M.A.; Amirkhani, A.; Parvin, F.; Chowdhury, D.; Molloy, M.P.; Deva, A.K.; Vickery, K.; Hu, H. One step forward with dry surface biofilm (DSB) of *Staphylococcus aureus*: TMT-based quantitative proteomic analysis reveals proteomic shifts between DSB and hydrated biofilm. *Int. J. Mol. Sci.* **2022**, *23*, 12238. [CrossRef]
17. Rahman, M.A.; Amirkhani, A.; Chowdhury, D.; Mempin, M.; Molloy, M.P.; Deva, A.K.; Vickery, K.; Hu, H. Proteome of *Staphylococcus aureus* Biofilm Changes Significantly with Aging. *Int. J. Mol. Sci.* **2022**, *23*, 6415. [CrossRef] [PubMed]
18. Pfaffl, M.W. A new mathematical model for relative quantification in real-time RT–PCR. *Nucleic Acids Res.* **2001**, *29*, e45. [CrossRef]
19. Cheng, G.; Karunakaran, R.; East, A.K.; Poole, P.S. Multiplicity of sulfate and molybdate transporters and their role in nitrogen fixation in *Rhizobium leguminosarum* bv. viciae Rlv3841. *Mol. Plant-Microbe Interact.* **2016**, *29*, 143–152. [CrossRef]
20. Vandenesch, F.; Lina, G.; Henry, T. *Staphylococcus aureus* hemolysins, bi-component leukocidins, and cytolytic peptides: A redundant arsenal of membrane-damaging virulence factors? *Front. Cell. Infect. Microbiol.* **2012**, *2*, 12. [CrossRef]
21. Shah, P.; Swiatlo, E. A multifaceted role for polyamines in bacterial pathogens. *Mol. Microbiol.* **2008**, *68*, 4–16. [CrossRef] [PubMed]

22. Antognoni, F.; Del Duca, S.; Kuraishi, A.; Kawabe, E.; Fukuchi-Shimogori, T.; Kashiwagi, K.; Igarashi, K. Transcriptional inhibition of the operon for the spermidine uptake system by the substrate-binding protein PotD. *J. Biol. Chem.* **1999**, *274*, 1942–1948. [CrossRef]
23. Atshan, S.S.; Shamsudin, M.N.; Lung, T.; Than, L.; Sekawi, Z.; Ghaznavi-Rad, E.; Pei Pei, C. Comparative characterisation of genotypically different clones of MRSA in the production of biofilms. *BioMed Res. Int.* **2012**, *2012*, 417247. [CrossRef]
24. da Silva, W.M.; Bei, J.; Amigo, N.; Valacco, P.; Amadio, A.F.; Zhang, Q.; Wu, X.; Larzábal, M.; Chen, Z.; Cataldi, A. Quantification of Enterohemorrhagic *Escherichia coli* O157: H7 proteome using TMT-Based Analysis. *bioRxiv* **2018**, 312652. [CrossRef]
25. Piras, C.; Di Ciccio, P.A.; Soggiu, A.; Greco, V.; Tilocca, B.; Costanzo, N.; Ceniti, C.; Urbani, A.; Bonizzi, L.; Ianieri, A.S. *aureus* biofilm protein expression linked to antimicrobial resistance: A proteomic study. *Animals* **2021**, *11*, 966. [CrossRef]
26. Parvin, F.; Rahman, M.A.; Deva, A.K.; Vickery, K.; Hu, H. *Staphylococcus aureus* cell wall phenotypic changes associated with biofilm maturation and water availability: A key contributing factor for chlorine resistance. *Int. J. Mol. Sci.* **2023**, *24*, 4983. [CrossRef]
27. Theodoulou, F.L.; Kerr, I.D. ABC transporter research: Going strong 40 years on. *Biochem. Soc. Trans.* **2015**, *43*, 1033–1040. [CrossRef]
28. Brady, R.A.; Leid, J.G.; Camper, A.K.; Costerton, J.W.; Shirtliff, M.E. Identification of *Staphylococcus aureus* proteins recognized by the antibody-mediated immune response to a biofilm infection. *Infect. Immun.* **2006**, *74*, 3415–3426. [CrossRef] [PubMed]
29. Islam, N.; Ross, J.M.; Marten, M.R. Proteome analyses of *Staphylococcus aureus* biofilm at elevated levels of NaCl. *Clin. Microbiol.* **2015**, *4*, 219.
30. Yang, J.; He, Y.; Jiang, J.; Chen, W.; Gao, Q.; Pan, L.; Shi, C. Comparative proteomic analysis by iTRAQ-2DLC-MS/MS provides insight into the key proteins involved in *Cronobacter* sp. biofilm formation. *Food Control* **2016**, *63*, 93–100. [CrossRef]
31. Branda, S.S.; González-Pastor, J.E.; Dervyn, E.; Ehrlich, S.D.; Losick, R.; Kolter, R. Genes involved in formation of structured multicellular communities by *Bacillus subtilis*. *J. Bacteriol.* **2004**, *186*, 3970–3979. [CrossRef] [PubMed]
32. Crowley, R.; Leigh, J.; Ward, P.; Lappin-Scott, H.; Bowler, L. Differential protein expression in *Streptococcus uberis* under planktonic and biofilm growth conditions. *Appl. Environ. Microbiol.* **2011**, *77*, 382–384. [CrossRef] [PubMed]
33. Hinsa, S.M.; Espinosa-Urgel, M.; Ramos, J.L.; O'toole, G.A. Transition from reversible to irreversible attachment during biofilm formation by *Pseudomonas fluorescens* WCS365 requires an ABC transporter and a large secreted protein. *Mol. Microbiol.* **2003**, *49*, 905–918. [CrossRef] [PubMed]
34. Vanderlinde, E.M.; Harrison, J.J.; Muszyński, A.; Carlson, R.W.; Turner, R.J.; Yost, C.K. Identification of a novel ABC transporter required for desiccation tolerance, and biofilm formation in *Rhizobium leguminosarum* bv. viciae 3841. *FEMS Microbiol. Ecol.* **2010**, *71*, 327–340. [CrossRef] [PubMed]
35. Zhu, X.; Long, F.; Chen, Y.; Knøchel, S.; She, Q.; Shi, X. A putative ABC transporter is involved in negative regulation of biofilm formation by Listeria monocytogenes. *Appl. Environ. Microbiol.* **2008**, *74*, 7675–7683. [CrossRef] [PubMed]
36. Beenken, K.E.; Dunman, P.M.; McAleese, F.; Macapagal, D.; Murphy, E.; Projan, S.J.; Blevins, J.S.; Smeltzer, M.S. Global gene expression in *Staphylococcus aureus* biofilms. *J. Bacteriol.* **2004**, *186*, 4665–4684. [CrossRef]
37. Vytvytska, O.; Nagy, E.; Blüggel, M.; Meyer, H.E.; Kurzbauer, R.; Huber, L.A.; Klade, C.S. Identification of vaccine candidate antigens of *Staphylococcus aureus* by serological proteome analysis. *Proteomics* **2002**, *2*, 580–590. [CrossRef]
38. Speziale, P.; Pietrocola, G. The multivalent role of fibronectin-binding proteins A and B (FnBPA and FnBPB) of *Staphylococcus aureus* in host infections. *Front. Microbiol.* **2020**, *11*, 572022. [CrossRef]
39. Hofbauer, B.; Vomacka, J.; Stahl, M.; Korotkov, V.S.; Jennings, M.C.; Wuest, W.M.; Sieber, S.A. Dual Inhibitor of *Staphylococcus aureus* Virulence and Biofilm Attenuates Expression of Major Toxins and Adhesins. *Biochemistry* **2018**, *57*, 1814–1820. [CrossRef]
40. Kot, B.; Sytykiewicz, H.; Sprawka, I. Expression of the Biofilm-Associated Genes in Methicillin-Resistant *Staphylococcus aureus* in Biofilm and Planktonic Conditions. *Int. J. Mol. Sci.* **2018**, *19*, 3487. [CrossRef]
41. Paharik, A.E.; Horswill, A.R. The Staphylococcal Biofilm: Adhesins, Regulation, and Host Response. *Microbiol. Spectr.* **2016**, *4*, 2. [CrossRef] [PubMed]
42. Ibberson, C.B.; Parlet, C.P.; Kwiecinski, J.; Crosby, H.A.; Meyerholz, D.K.; Horswill, A.R. Hyaluronan modulation impacts *Staphylococcus aureus* biofilm infection. *Infect. Immun.* **2016**, *84*, 1917–1929. [CrossRef] [PubMed]
43. Rahman, M.A.; Choi, Y.H.; Pradeep, G.; Yoo, J.C. An ammonium sulfate sensitive chitinase from *Streptomyces* sp. CS501. *Arch. Pharmacal Res.* **2014**, *37*, 1522–1529. [CrossRef] [PubMed]
44. Boles, B.R.; Horswill, A.R. Agr-mediated dispersal of *Staphylococcus aureus* biofilms. *PLoS Pathog.* **2008**, *4*, e1000052. [CrossRef]
45. Periasamy, S.; Joo, H.-S.; Duong, A.C.; Bach, T.-H.L.; Tan, V.Y.; Chatterjee, S.S.; Cheung, G.Y.; Otto, M. How *Staphylococcus aureus* biofilms develop their characteristic structure. *Proc. Natl. Acad. Sci. USA* **2012**, *109*, 1281–1286. [CrossRef] [PubMed]
46. Resch, A.; Rosenstein, R.; Nerz, C.; Götz, F. Differential gene expression profiling of *Staphylococcus aureus* cultivated under biofilm and planktonic conditions. *Appl. Environ. Microbiol.* **2005**, *71*, 2663–2676. [CrossRef]
47. Kantyka, T.; Plaza, K.; Koziel, J.; Florczyk, D.; Stennicke, H.R.; Thogersen, I.B.; Enghild, J.J.; Silverman, G.A.; Pak, S.C.; Potempa, J. Inhibition of *Staphylococcus aureus* cysteine proteases by human serpin potentially limits staphylococcal virulence. *Biol. Chem.* **2011**, *392*, 483–489. [CrossRef]
48. Martínez-García, S.; Peralta, H.; Betanzos-Cabrera, G.; Chavez-Galan, L.; Rodríguez-Martínez, S.; Cancino-Diaz, M.E.; Cancino-Diaz, J.C. Proteomic comparison of biofilm vs. planktonic *Staphylococcus epidermidis* cells suggests key metabolic differences between these conditions. *Res. Microbiol.* **2021**, *172*, 103796. [CrossRef]

49. Chen, X.; Wu, H.; Cao, Y.; Yao, X.; Zhao, L.; Wang, T.; Yang, Y.; Lv, D.; Chai, Y.; Cao, Y. Ion-pairing chromatography on a porous graphitic carbon column coupled with time-of-flight mass spectrometry for targeted and untargeted profiling of amino acid biomarkers involved in *Candida albicans* biofilm formation. *Mol. BioSystems* **2014**, *10*, 74–85. [CrossRef]
50. Wall, E.A.; Caufield, J.H.; Lyons, C.E.; Manning, K.A.; Dokland, T.; Christie, G.E. Specific N-terminal cleavage of ribosomal protein L 27 in *Staphylococcus aureus* and related bacteria. *Mol. Microbiol.* **2015**, *95*, 258–269. [CrossRef]
51. Weiss, A.; Moore, B.D.; Tremblay, M.H.; Chaput, D.; Kremer, A.; Shaw, L.N. The ω subunit governs RNA polymerase stability and transcriptional specificity in *Staphylococcus aureus*. *J. Bacteriol.* **2017**, *199*, e00459-16. [CrossRef] [PubMed]
52. Li, S.; Li, H.; Qi, T.; Yan, X.; Wang, B.; Guan, J.; Li, Y. Comparative transcriptomics analyses of the different growth states of multidrug-resistant *Acinetobacter baumannii*. *Biomed. Pharmacother.* **2017**, *85*, 564–574. [CrossRef] [PubMed]
53. Xu, K.D.; Franklin, M.J.; Park, C.-H.; McFeters, G.A.; Stewart, P.S. Gene expression and protein levels of the stationary phase sigma factor, RpoS, in continuously-fed *Pseudomonas aeruginosa* biofilms. *FEMS Microbiol. Lett.* **2001**, *199*, 67–71. [CrossRef] [PubMed]
54. Li, W.; Yao, Z.; Sun, L.; Hu, W.; Cao, J.; Lin, W.; Lin, X. Proteomics analysis reveals a potential antibiotic cocktail therapy strategy for *Aeromonas hydrophila* infection in biofilm. *J. Proteome Res.* **2016**, *15*, 1810–1820. [CrossRef] [PubMed]
55. Weber, H.; Engelmann, S.; Becher, D.; Hecker, M. Oxidative stress triggers thiol oxidation in the glyceraldehyde-3-phosphate dehydrogenase of *Staphylococcus aureus*. *Mol. Microbiol.* **2004**, *52*, 133–140. [CrossRef]
56. Oliveira, L.; Madureira, P.; Andrade, E.B.; Bouaboud, A.; Morello, E.; Ferreira, P.; Poyart, C.; Trieu-Cuot, P.; Dramsi, S. Group B streptococcus GAPDH is released upon cell lysis, associates with bacterial surface, and induces apoptosis in murine macrophages. *PLoS ONE* **2012**, *7*, e29963. [CrossRef] [PubMed]
57. Planchon, S.; Desvaux, M.; Chafsey, I.; Chambon, C.; Leroy, S.; Hébraud, M.; Talon, R. Comparative subproteome analyses of planktonic and sessile *Staphylococcus xylosus* C2a: New insight in cell physiology of a coagulase-negative *Staphylococcus* in biofilm. *J. Proteome Res.* **2009**, *8*, 1797–1809. [CrossRef] [PubMed]
58. Wang, Y.; Yi, L.; Wu, Z.; Shao, J.; Liu, G.; Fan, H.; Zhang, W.; Lu, C. Comparative proteomic analysis of *Streptococcus suis* biofilms and planktonic cells that identified biofilm infection-related immunogenic proteins. *PLoS ONE* **2012**, *7*, e33371. [CrossRef] [PubMed]
59. Foulston, L.; Elsholz, A.K.; DeFrancesco, A.S.; Losick, R. The extracellular matrix of *Staphylococcus aureus* biofilms comprises cytoplasmic proteins that associate with the cell surface in response to decreasing pH. *MBio* **2014**, *5*, e01667-14. [CrossRef]
60. Gil, C.; Solano, C.; Burgui, S.; Latasa, C.; García, B.; Toledo-Arana, A.; Lasa, I.; Valle, J. Biofilm Matrix Exoproteins Induce a Protective Immune Response against *Staphylococcus aureus* Biofilm Infection. *Infect. Immun.* **2014**, *82*, 1017–1029. [CrossRef]
61. Zhang, J.; Meng, L.; Zhang, Y.; Sang, L.; Liu, Q.; Zhao, L.; Liu, F.; Wang, G. GapB is involved in biofilm formation dependent on LrgAB but not the SinI/R system in *Bacillus cereus* 0-9. *Front. Microbiol.* **2020**, *11*, 591926. [CrossRef] [PubMed]
62. Stewart, P.S.; Zhang, T.; Xu, R.; Pitts, B.; Walters, M.C.; Roe, F.; Kikhney, J.; Moter, A. Reaction–diffusion theory explains hypoxia and heterogeneous growth within microbial biofilms associated with chronic infections. *Npj Biofilms Microbiomes* **2016**, *2*, 16012. [CrossRef] [PubMed]
63. Walters, M.C.; Roe, F.; Bugnicourt, A.; Franklin, M.J.; Stewart, P.S. Contributions of antibiotic penetration, oxygen limitation, and low metabolic activity to tolerance of *Pseudomonas aeruginosa* biofilms to ciprofloxacin and tobramycin. *Antimicrob. Agents Chemother.* **2003**, *47*, 317–323. [CrossRef]
64. Borriello, G.; Werner, E.; Roe, F.; Kim, A.M.; Ehrlich, G.D.; Stewart, P.S. Oxygen limitation contributes to antibiotic tolerance of *Pseudomonas aeruginosa* in biofilms. *Antimicrob. Agents Chemother.* **2004**, *48*, 2659–2664. [CrossRef]
65. Zheng, Z.; Stewart, P.S. Growth limitation of *Staphylococcus epidermidis* in biofilms contributes to rifampin tolerance. *Biofilms* **2004**, *1*, 31–35. [CrossRef]
66. Eng, R.; Padberg, F.; Smith, S.; Tan, E.; Cherubin, C. Bactericidal effects of antibiotics on slowly growing and nongrowing bacteria. *Antimicrob. Agents Chemother.* **1991**, *35*, 1824–1828. [CrossRef] [PubMed]
67. Evans, D.; Allison, D.; Brown, M.; Gilbert, P. Susceptibility of Pseudomonas aeruginosa and *Escherichia coli* biofilms towards ciprofloxacin: Effect of specific growth rate. *J. Antimicrob. Chemother.* **1991**, *27*, 177–184. [CrossRef] [PubMed]
68. Eschbach, M.; Schreiber, K.; Trunk, K.; Buer, J.; Jahn, D.; Schobert, M. Long-term anaerobic survival of the opportunistic pathogen *Pseudomonas aeruginosa* via pyruvate fermentation. *J. Bacteriol.* **2004**, *186*, 4596–4604. [CrossRef] [PubMed]
69. Zhu, Y.; Weiss, E.C.; Otto, M.; Fey, P.D.; Smeltzer, M.S.; Somerville, G.A. *Staphylococcus aureus* biofilm metabolism and the influence of arginine on polysaccharide intercellular adhesin synthesis, biofilm formation, and pathogenesis. *Infect. Immun.* **2007**, *75*, 4219–4226. [CrossRef]
70. Sambanthamoorthy, K.; Schwartz, A.; Nagarajan, V.; Elasri, M.O. The role of msa in *Staphylococcus aureus* biofilm formation. *BMC Microbiol.* **2008**, *8*, 221. [CrossRef]
71. Klein, M.I.; Xiao, J.; Lu, B.; Delahunty, C.M.; Yates, J.R., III; Koo, H. Streptococcus mutans Protein Synthesis during Mixed-Species Biofilm Development by High-Throughput Quantitative Proteomics. *PLoS ONE* **2012**, *7*, e45795. [CrossRef] [PubMed]
72. Brady, R.A.; May, G.A.; Leid, J.G.; Prior, M.L.; Costerton, J.W.; Shirtliff, M.E. Resolution of *Staphylococcus aureus* Biofilm Infection Using Vaccination and Antibiotic Treatment. *Infect. Immun.* **2011**, *79*, 1797. [CrossRef] [PubMed]

73. Chew, J.; Zilm, P.S.; Fuss, J.M.; Gully, N.J. A proteomic investigation of *Fusobacterium nucleatum* alkaline-induced biofilms. *BMC Microbiol.* **2012**, *12*, 189. [CrossRef] [PubMed]
74. Perez-Riverol, Y.; Bai, J.; Bandla, C.; García-Seisdedos, D.; Hewapathirana, S.; Kamatchinathan, S.; Kundu, D.J.; Prakash, A.; Frericks-Zipper, A.; Eisenacher, M. The PRIDE database resources in 2022: A hub for mass spectrometry-based proteomics evidences. *Nucleic Acids Res.* **2022**, *50*, D543–D552. [CrossRef] [PubMed]